Electronic Supplementary Information (ESI)

for

Hydrophilic $Cu_{2-x}Se$/reduced graphene oxide nanocomposites with tunable plasmonic properties and their applications in cellular dark-field microscopic imaging

Wen Long Li, [a] Shao Qing Lie, [a] Yu Qing Du, [b] Xiao Yan Wan, [b] Ting Ting Wang, [b] Jian Wang, [b] Cheng Zhi Huang * [a b]

a Key Laboratory of Luminescent and Real-Time Analytical Chemistry (Southwest University), Ministry of Education, College of Chemistry and Chemical Engineering, Southwest University, Chongqing 400715, China

b College of Pharmaceutical Science, Southwest University, Chongqing 400715, China

* Corresponding Author. E-mail: chengzhi@swu.edu.cn

EXPERIMENTAL SECTION

Chemicals and Materials. Graphene oxide (GO) was purchased from XF NANO INC (Nanjing, China) and dissolved in deionized water via sonication for several hours to obtain the GO aqueous solution. Ascorbic acid (AA) was obtained from Dingguo Changsheng Biotechnology Co., Ltd (Beijing, China). SeO_2 was supplied by Aladdin Chemistry Co., Ltd (Shanghai, China) and stored in a desiccator at room temperature. $CuSO_4 \cdot 5H_2O$ (Rgent Chemical Reagent Co., Ltd, Tianjin, China) was analytical grade. Polyvinylpyrrolidone (PVP, Mw = 55,000) was supplied by Aldrich Co.. Other reagents including ethanol, n-propanol, ethylene glycol, acetone, N, N-dimethylformide (DMF), and dimethyl sulfoxide (DMSO) were analytical reagent grade. All chemicals were used as received without further purification. Milli-Q purified water (18.2 $M\Omega \cdot cm^{-1}$) was used throughout the experiments.

Apparatus. The absorption spectra were recorded by a UV-3600 UV-vis-NIR spectrophotometer (Shimadzu, Japan). Transmission electron microscopy (TEM), high resolution transmission electron microscopy (HRTEM), and selected area electron diffraction (SAED) measurements were obtained from a Tecnai G2 F20 S-TWIN microscopy (FEI, USA). Scanning electron microscopy (SEM) and Energy-dispersive X-ray spectroscopy (EDS) was performed with an S-4800 scanning electron microscope (Hitachi, Japan). Atomic force microscopy (AFM) images were obtained using a Dimension Icon Scan Asyst atomic force microscope (Bruker Co.). X-ray photoelectron spectroscopy (XPS) analysis was conducted by an ESCALAB 250 X-ray photoelectron spectrometer (Thermo, USA). X-Ray diffraction (XRD) analyses were carried out on an XRD-7000 with Cu Kα radiation source. A Fourier transform infrared (FT-IR) spectrophotometer (FTIR-8400S, Shimadzu, Japan) was employed to measuring the FT-IR spectrum. Raman spectra were investigated on a LabRAM HR800 Laser Raman spectroscopy (HORIBA Jobin Yvon CO. Ltd., France). Thermogravimetric analyses were performed in air using a TGA instrument (TA-STD 600, TA Instruments Inc., New Castle, USA). Dynamic light scattering (DLS) and ζ-potential measurements were performed using a Zatasizer Nano-ZS90 instrument (Malvern Inc).

Synthesis of $Cu_{2-x}Se$/rGO nanocomposites. Briefly, GO aqueous solution (10 mL, 0.1mg/mL) was magnetically stirred to form a homogeneous pale-yellow solution, in a water bath at 30 °C. Then, 50 μL SeO_2 (0.01 mmol) and 200 μL AA (0.01 g) was added into the above solution followed by continuous stirring for 10 min, with an obvious color change from pale-yellow to orange. Further, 50 μL $CuSO_4$ (0.02 mmol) and 800 μL AA (0.04 g) was added, and the resulting mixture was sustained stirring for 10 h upon air exposure. The products in the yellow-green dispersion were centrifuged for 10 min at 8000 rpm and washed thrice with distilled water, and redispersed in water for characterization and further use. $Cu_{2-x}Se$/rGO nanocomposites with different x value (from $x \approx 0$ to $x = 0.67$) were obtained for different reaction time.

Pure $Cu_{2-x}Se$ NPs were performed with the use of 10 mL distilled water, containing 10 mg PVP (Mw = 55,000), instead of 10 mL 0.1mg/mL GO solution.

Cell viability. HEp-2 cells were cultured in Minimal Essential Medium (MEM) supplemented with 10 % (v/v) fetal bovine serum (FBS) at 37 °C in a humidified incubator of 5 % CO_2. The suspension of HEp-2 cells (2×10^5 cells per well) was added in the 96-well plates to let cells be seeded for 24 hours before incubation. $Cu_{2-x}Se$/rGO nanocomposites were introduced separately to each well with different test concentrations (0.1, 0.5, 1, 5, 10, 25, 50, 100 μg/mL) in culture medium. Cells cultured in the medium without adding $Cu_{2-x}Se$/rGO nanocomposites were taken as control. After 24 h incubation, the cells were washed with PBS buffer solution twice. 10 μL of CCK-8 solution was added to each well and incubated for an additional 1 h. The optical density (OD) of each well was recorded on a Microplate Reader at 450 nm. The cell viability is expressed following the below equation:

$$\text{Cell viability (\%)} = (\text{OD test} - \text{OD blank}) / (\text{OD control} - \text{OD blank})$$

where OD test is the OD of the cells exposed to $Cu_{2-x}Se$/rGO sample, OD control is the OD of the control sample, and OD blank is the OD of the wells without HEp-2 cells.

Dark-Field Microscopic Imaging (iDFM) of $Cu_{2-x}Se$/rGO nanocomposites on Cancer Cells. 100 μL suspension of HEp-2 cells (about 10^4 cells / mL) in Minimal

Essential Medium (MEM) supplemented with 10 % fetal bovine serum (FBS) was plated onto a glass coverslip (1.5×1.5 cm^2) in a 12-well plates, cultured for 24 h in an incubator (37 °C, 5 % CO_2), and then treated with the $Cu_{2-x}Se$/rGO nanocomposites solution for another 24 h. The resulting solution was rinsed with PBS buffer for 3 times and then fixed with 4 % paraformaldehyde. Afterwards, the final mixture was sealed with glycerol. Dark-field light scattering images were acquired using an Olympus BX-51 Microscope (Tokyo, Japan) with a high numerical-aperture dark-field condenser (U-DCW, 1.2-1.4) for illumination and a 40× objective (UPLANFLN, numerical aperture = 0.6-1.3) for subsequent collection of the scattered light. The colorful dark-field images were recorded with a DP72 single-chip color CCD camera (Olympus, Japan).

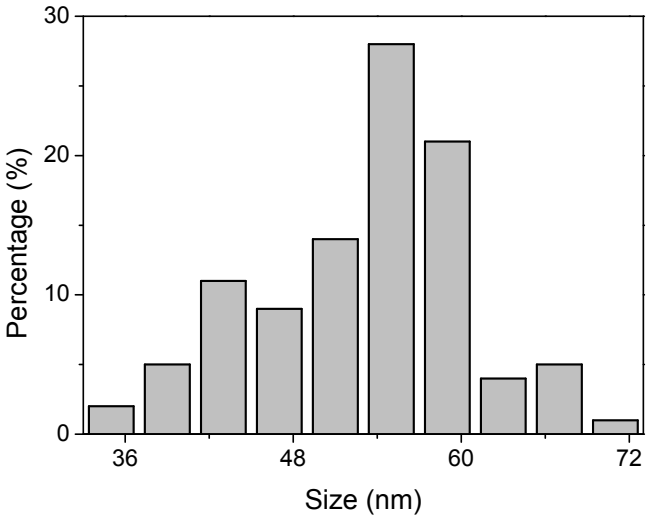

Fig. S1. Particle size distribution histogram diagram of $Cu_{2-x}Se$ NPs on the surface of rGO sheets. The size distribution of $Cu_{2-x}Se$ NPs on rGO sheets was obtained by measuring the nanoparticle diameters in TEM image (Fig. 1C).

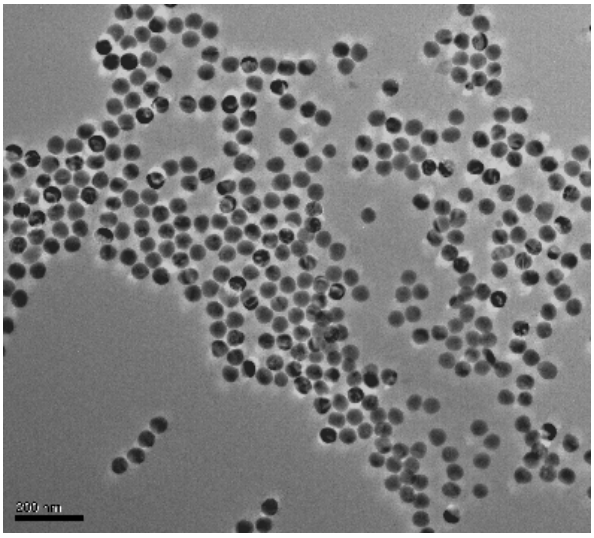

Fig. S2. A typical TEM image of pure $Cu_{2-x}Se$ NPs capped by PVP (Mw = 55,000). The scale bar indicates 200 nm.

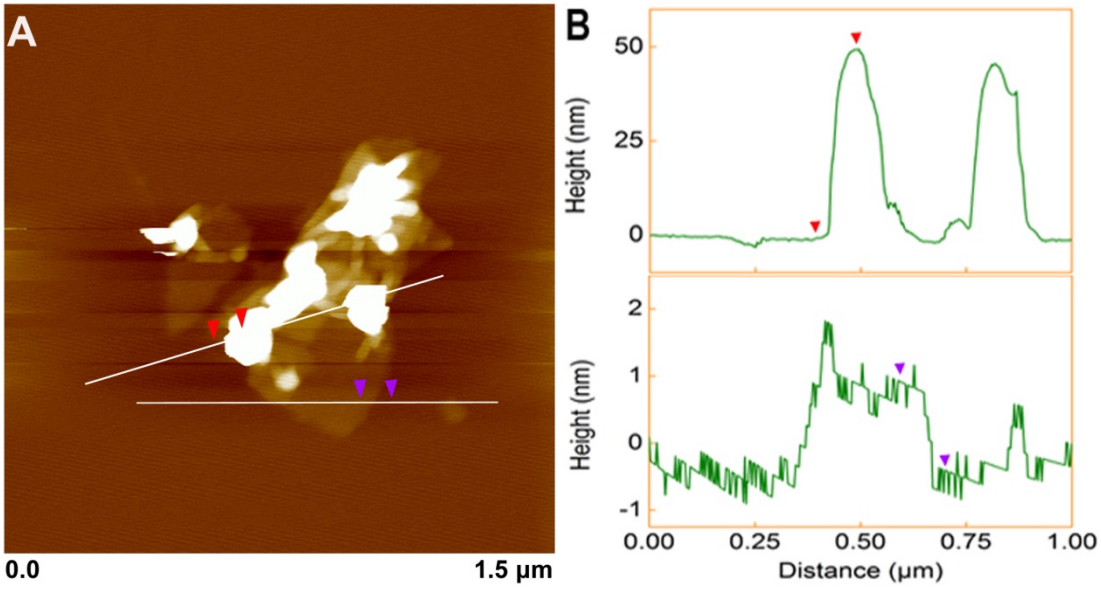

Fig. S3. (A) AFM image and (B) the cross section analysis of $Cu_{2-x}Se$/rGO nanocomposites. The cross section analysis of AFM illustrates an apparent thickness of ~1 nm for rGO and a diameter of ~50 nm for $Cu_{2-x}Se$ NPs, close to the result of TEM image.

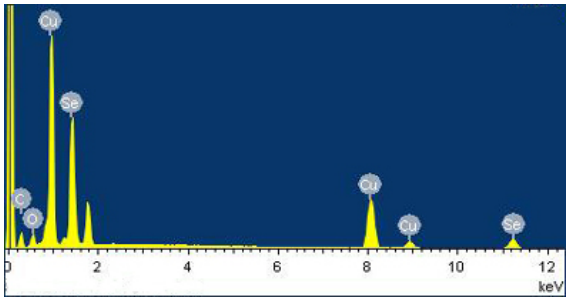

Element	Weight (%)	Atomic (%)
C K	24.02	58.24
O K	7.28	13.24
Cu K	35.54	16.29
Se L	33.17	12.23
Cu/Se		1.33

Fig. S4. EDX spectrum of as-prepared $Cu_{2-x}Se$/rGO nanocomposites. It clearly confirms the presence of Cu, Se, C and O elements.

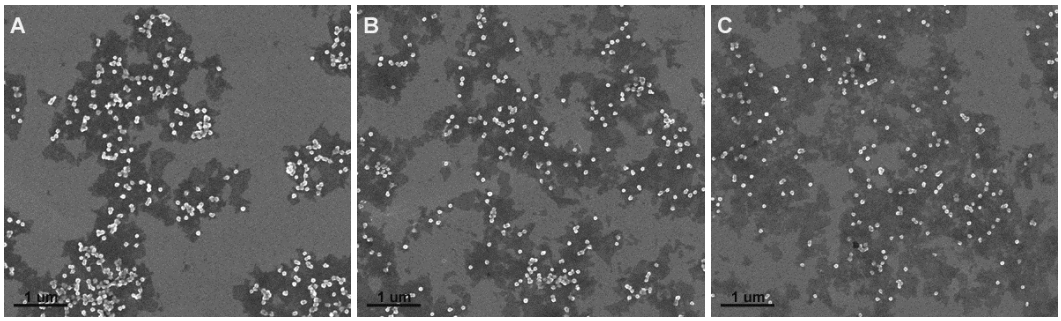

Fig. S5. SEM images of rGO sheets with different assembly densities of $Cu_{2-x}Se$ NPs, for (A) 0.1 mg/mL, (B) 0.2 mg/mL, and (C) 0.3 mg/mL of GO, respectively. The scale bars indicate 1 μm.

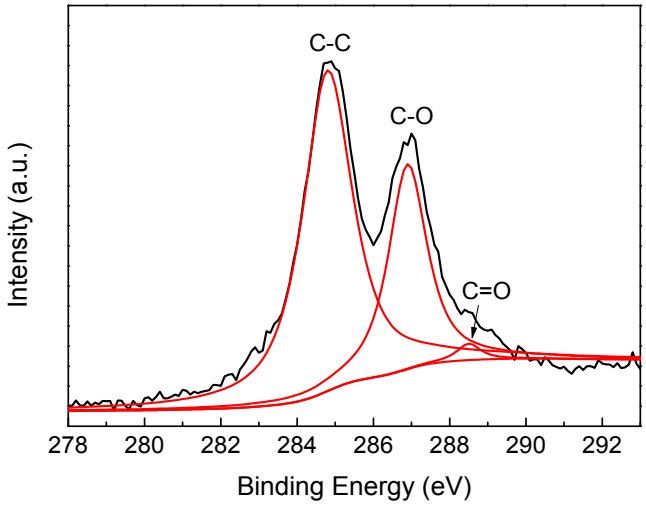

Fig. S6. XPS spectrum of C 1s of $Cu_{2-x}Se$/rGO nanocomposites. The peaks correspond to C-C, C-O (epoxy and alkoxy) and C=O (carbonyl), respectively.

The heat stability of $Cu_{2-x}Se$/rGO nanocomposites

As displayed in Fig. S7, the abrupt mass loss of GO takes place around 200 °C, attributed to the decomposition of the most labile oxygen functionalities. The slow, steady mass loss above 300 °C can be ascribed to desorption of more stable oxygen-containing functional groups. Removal of adsorbed water accounts for the mass loss below 100 ℃.[1] Compared with GO, the as-prepared $Cu_{2-x}Se$/rGO nanocomposites exhibit higher thermal stability and the mass loss at about 200 °C decreases dramatically, indicating the efficient removal of the labile oxygen functionalities. However, the mass loss above 300 °C still exists, suggesting that the most stable oxygen- containing functional groups were reserved.

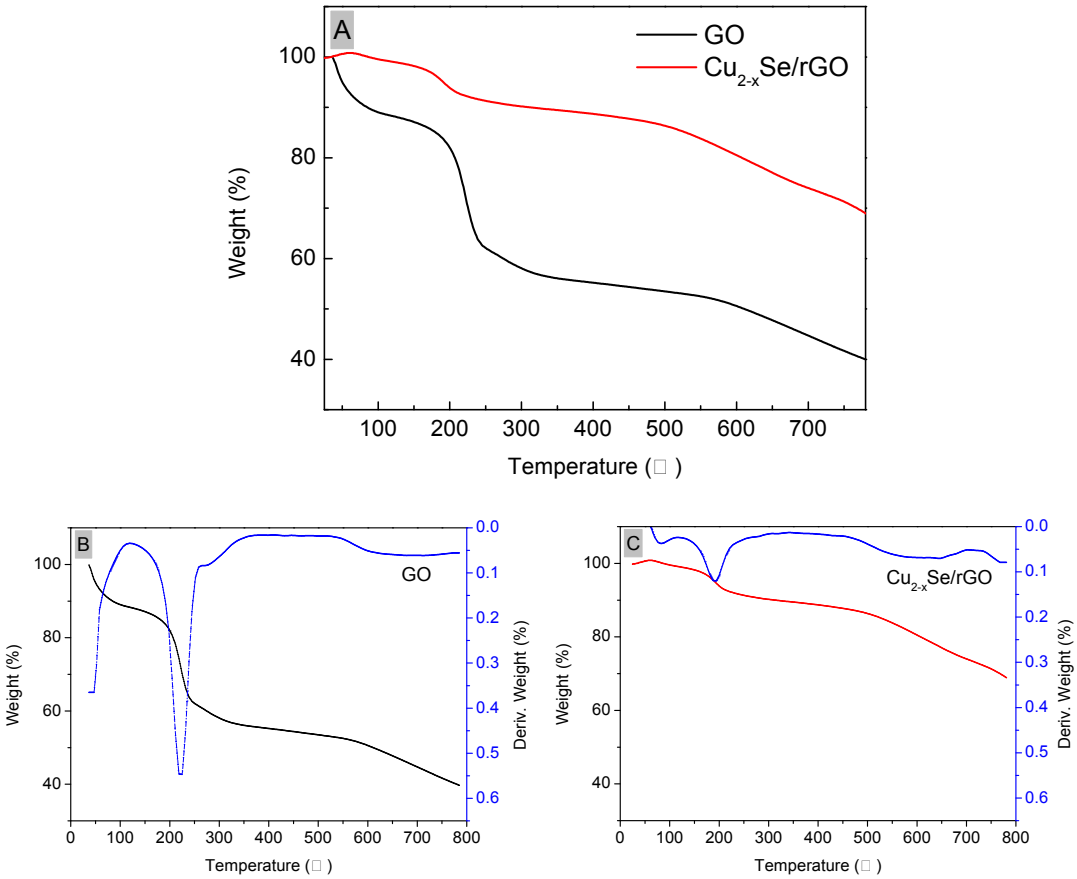

Fig. S7. (A) Typical TGA and DTG curves of (B) GO and (C) $Cu_{2-x}Se$/rGO nanocomposites. Thermogravimetric analysis (TGA) were performed in air with a ramp of 10 ℃/min up to 780 ℃.

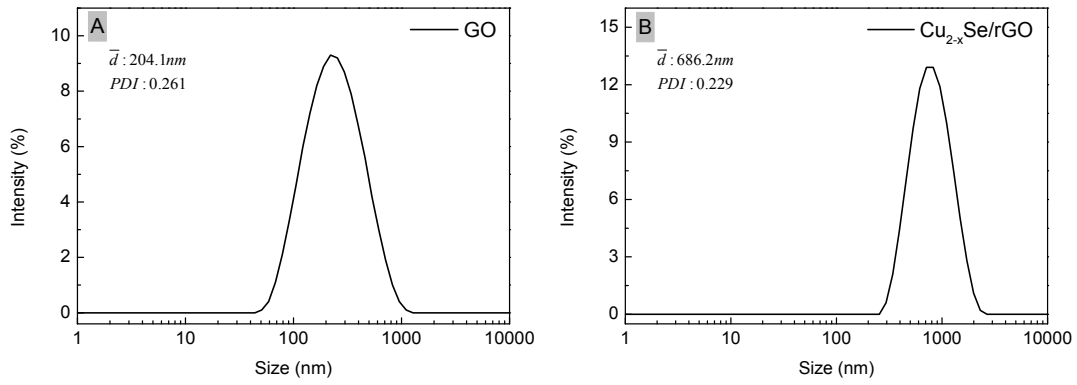

Fig. S8. DLS spectra of (A) GO and (B) $Cu_{2-x}Se$/rGO nanocomposites. The average hydrodynamics diameter of GO is 204.1 nm (the PDI is 0.261), and $Cu_{2-x}Se$/rGO nanocomposites is 686.2 nm (the PDI is 0.229), which indicate the size distributions of GO and $Cu_{2-x}Se$/rGO nanocomposites are relatively homogeneous. (PDI is polydispersity index)

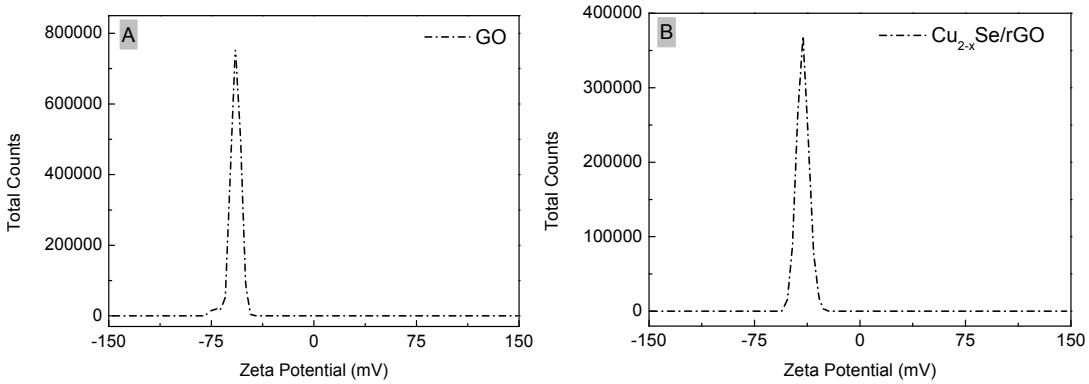

Fig. S9. ζ-potential spectra of (A) GO and (B) $Cu_{2-x}Se$/rGO nanocomposites. The main potential of GO is -57.4 mV (the conductivity is 0.00831 mS/cm), and $Cu_{2-x}Se$/rGO nanocomposites is -40.6 mV (the conductivity is 0.0105 mS/cm). Neither splitted nor disordered peak was found in each spectrum, which reveals the surface charge is pure.

The dispersion stability of $Cu_{2-x}Se$/rGO nanocomposites

It is worthwhile mentioning that no additional capping reagents were added in this study, unlike other reports. Nevertheless, $Cu_{2-x}Se$/rGO nanocomposites can be suspended stably in aqueous solution at room temperature for several days. The oxidized products of AA may play a critical role in the stabilization of $Cu_{2-x}Se$/rGO nanocomposites. It is well known that an AA molecule can transform into dehydroascorbic acid via loss of two protons (deprotonation).[2] The dehydroascorbic acid can be further converted into oxalic and guluronic acids. The rGO decorated with $Cu_{2-x}Se$ NPs may also have some residual oxygen functionalities, such as hydroxyl and epoxy groups (Fig. 3A). Thus, guluronic acid or oxalic acids might form hydrogen bonds with the residual oxygen functionalities on the rGO surfaces.[3] Such interactions can disrupt the π-π stacking between the rGO sheets, and further prevent the formation of the agglomerates. In addition, the $Cu_{2-x}Se$ NPs anchored on rGO sheets prevent the rGO sheets from direct stacking after the reduction of GO, which also avoid the aggregation.

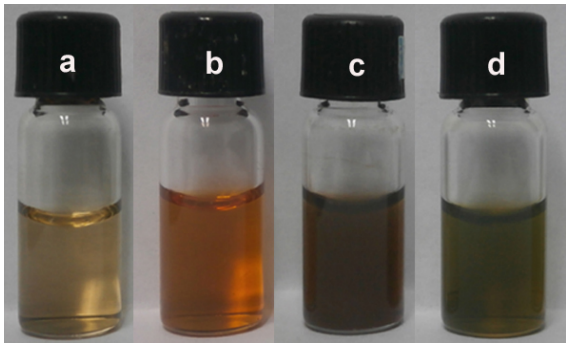

Fig. S10. Photographs of aqueous dispersions of (a) GO, (b) Se/GO, (c) Cu_2Se/GO and (d) $Cu_{2-x}Se$/rGO nanocomposites.

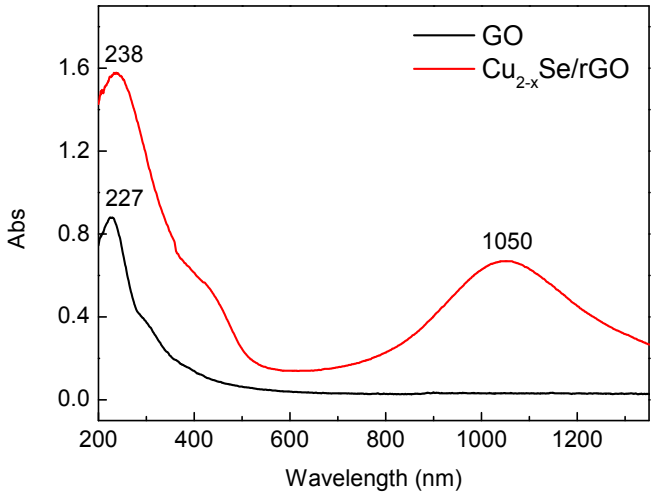

Fig. S11. Absorption spectra of GO and $Cu_{2-x}Se$/rGO nanocomposites. It is clearly seen that an intense NIR absorption occurs in $Cu_{2-x}Se$/rGO nanocomposites.

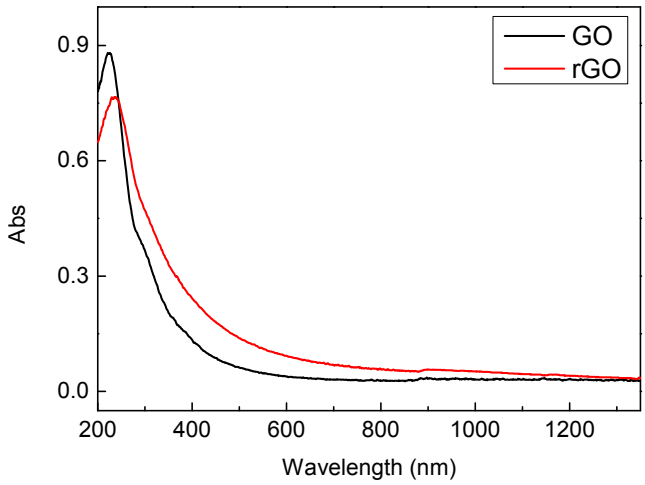

Fig. S12. Optical Absorption spectra of GO and rGO. (rGO was obtained by graphene oxide

reduced via AA at 30℃ for 10 h).

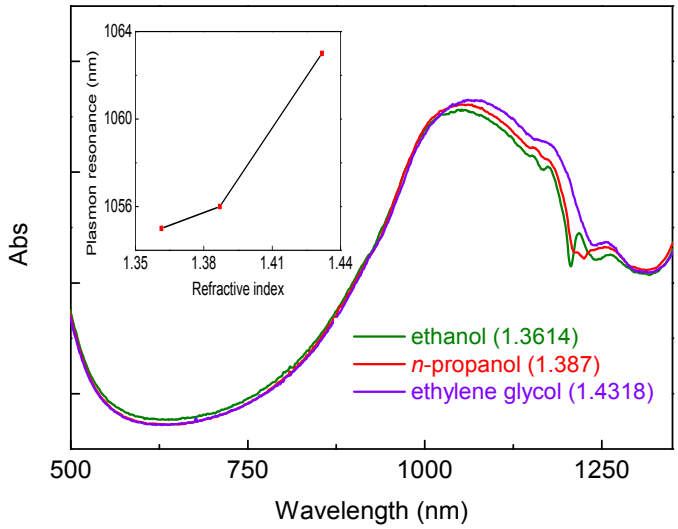

Fig. S13. Absorption spectra of $Cu_{2-x}Se$/rGO nanocomposites in different organic solvents: ethanol, *n*-propanol, and ethylene glycol with refractive indices of 1.3614, 1.387, and 1.4318, respectively. The inset shows the LSPR red-shifts with increasing refractive index of the solvent.

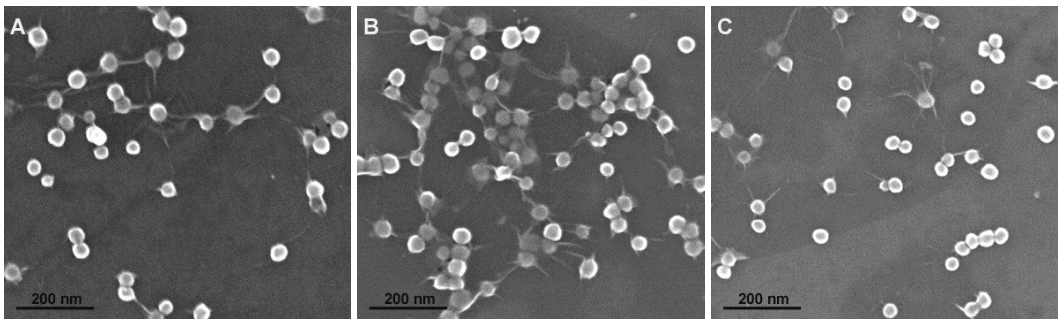

Fig. S14. SEM images of $Cu_{2-x}Se$/rGO nanocomposites synthesized for (A) 2 min, (B) 1 h, and (C) 10 h, respectively. The shape and size of $Cu_{2-x}Se$ NPs were preserved during the reaction. The scale bars indicate 200 nm.

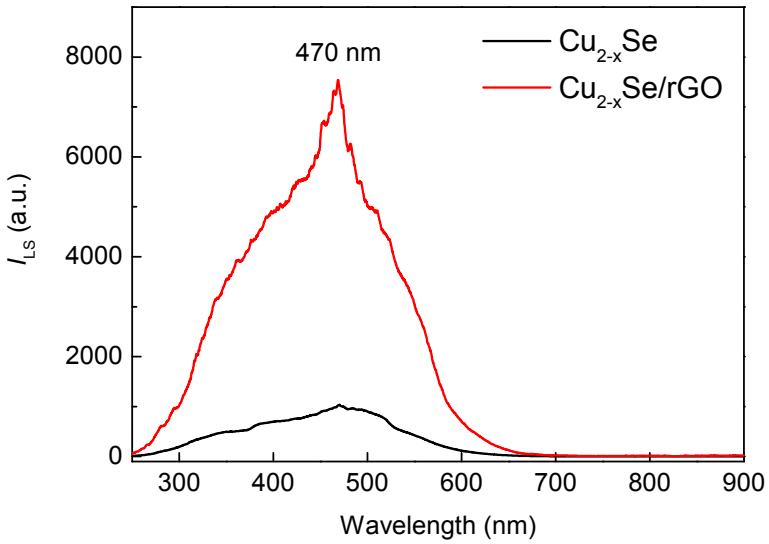

Fig. S15. The corresponding light scattering spectra of $Cu_{2-x}Se$ and $Cu_{2-x}Se$/rGO nanocomposites.

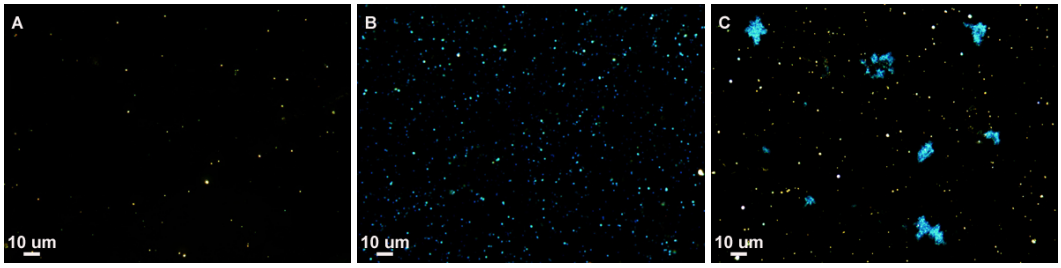

Fig. S16. Dark field light scattering images of (A) GO, (B) $Cu_{2-x}Se$, and (C) $Cu_{2-x}Se$/rGO nanocomposites. (The bright spots in the horizons come from the impurities on the glass slides.)

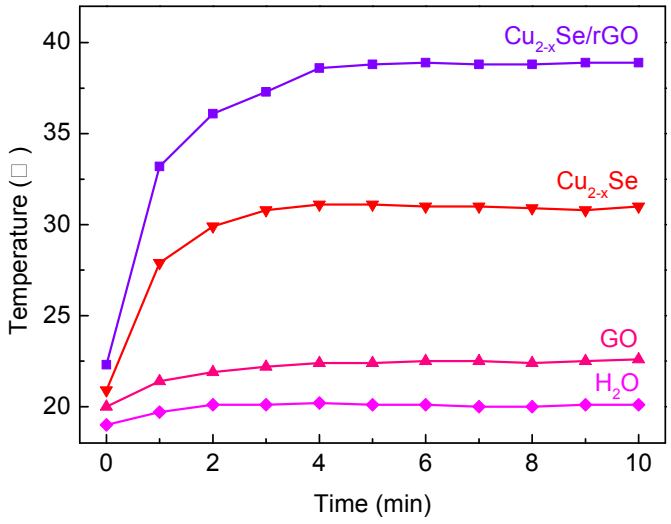

Fig. S17. Temperature profiles of pure water and aqueous dispersions of GO, $Cu_{2-x}Se$, Cu_{2-}

$_x$Se/rGO as a function of irradiation time (0 ~ 10 min) when illuminated with a 785 nm laser at a power of 0.6 W/cm^2.

References:

1. M. J. Fernández-Merino, L. Guardia, J. I. Paredes, S. Villar-Rodil, P. Solís-Fernández, A. Martínez-Alonso and J. M. D. Tascón, *J. Phys. Chem. C*, 2010, **114**, 6426-6432.
2. M. B. Davies, J. Austin and D. A. Partridge, *Vitamin C: Its Chemistry and Biochemistry*, The Royal Society of Chemistry, UK, 1991, 74-96.
3. J. Zhang, H. Yang, G. Shen, P. Cheng, J. Zhang and S. Guo, *Chem Commun*, 2010, **46**, 1112-1114.